Indian Journal of Experimental Biology
Vol. 58, September 2020, pp. 597-608

Pathological studies on *Pteris cretica* (L.) fern-Bovine Papilloma Virus infection in Syrian Golden Hamsters (*Mesocricetus auratus*)

Babu Lal Jangir[1#], DR Lauren[2] & R Somvanshi[1]*

[1]Division of Pathology, ICAR-Indian Veterinary Research Institute, Izatnagar-243 122, Uttar Pradesh, India
[2]Plant and Food Research Ruakura, Waikato Mail Centre, Hamilton 3240, New Zealand

Received 13 March 2019; *revised 29 April 2020*

Pteris cretica (L.) commonly known as Cretan brake is widely distributed in nature and considered as potential environmental carcinogen. However, only limited literature is available on this fern commonly taken by cattle while grazing. It is known that in cattle Bovine papilloma virus (BPV) induced benign tumours are converted into malignant with interaction of ptaquiloside (Pta) present in ferns. In the present investigation, we evaluated the pathological effects of *P. cretica* (PC)-BPV infection in laboratory model hamster. Though toxic principle Pta was detected in fern samples but quercetin could not be found. Tumours were successfully induced in hamsters by cutaneous wart suspension and histopathologically diagnosed as fibroma and lipofibroma. Histopathologically, hamsters showed mild to moderate vascular changes in vital organs, multiple cysts, degenerative changes, bile duct hyperplasia and necrosis in liver, haemorrhages and haemosiderosis in spleen, hypersecretory activity and prominent Peyer's patches in ileum, degenerative changes and presence of eosinophilic casts in renal tubules. Ultrastructural study revealed apoptosis in hepatocytes, abundance of variable shaped mitochondria in renal tubular lining epithelial cells and enterocytes showed abundance of mitochondria and cytoplasmolysis in the fern fed groups. Almost all the hamsters from BPV, fern and virus infection (PC+BPV) groups developed similar type of tumorous growths. The visible growths in the hamsters of these groups were either single or double large sized except multiple tumorous growths in one hamster from PC+BPV group. However, multiple palpable subcutaneous nodules were developed at the site of scarification in all the hamsters of BPV and PC+BPV groups. Our findings suggest that the Pta containing *P. cretica* feeding induced hepatotoxic and nephrotoxic lesions in hamsters, but effects of *P. cretica*-BPV infection were found negligible.

Keywords: BPV infection, Cattle grazing, Carcinogen, Cretan brake, Fibroma, Hepatotoxic, Nephrotoxic, Peyer's patches, Ptaquiloside, Tumour

Ferns constitute bulk of the vegetation in grazing areas, orchards and road sides of temperate region and hilly tract. There are about 280 fern species. *Pteris* found in the tropics and sub-tropics. *Pteris cretica* (L.) has fronds that are divided deeply into many long, ribbon-like sections and it grows up to 45 cms high and forms masses of light green, evergreen or semi-evergreen foliage[1]. A variety of ferns including *Pteris cretica* contains most potent toxin ptaquiloside (Pta)[2]. Pta is a nor-sesquiterpenoid glycoside with clastogenic[3], mutagenic[4], teratogenic[5] and carcinogenic[6] properties. At places, it contains high concentrations of Pta, which is its major environmental carcinogen. It undergoes a series of reactions and produces a reactive aglycone dienone intermediate, inactive pterosin-B and DNA adducts. Among them, dienone is the ultimate carcinogen and activated at alkaline pH[7], which is considered as the reason for location of tumours in the urinary bladder of ruminants[8] and ileum of rats[9]. Another potential carcinogen present in bracken fern is quercetin, a well known mutagenic flavonoid[10] which has been found to be genotoxic and mutagenic but its role in carcinogenesis has not been studied extensively.

Bovine papilloma viruses (BPVs) infect cattle[11], buffaloes[11,12] and yaks[13]. It infects the cutaneous and mucosal epithelia inducing hyperplastic lesions in cattle and buffaloes. Studies indicate that upper gastrointestinal tract[14] and urinary bladder tumours[15] in cattle are associated with prolonged bracken fern ingestion and infection with BPV. However, only a few studies have been carried out on bracken fern and BPV infection in laboratory animal hamster. Cell free

*Correspondence:
E-mail: dr.rsomvanshi@gmail.com (RS);
drbabu.jangir@gmail.com (BLJ)
[#]Present add.: Department of Veterinary Pathology, College of Veterinary Sciences, Lala Lajpat Rai University of Veterinary and Animal Sciences, Hisar, Haryana, India

extract of cutaneous warts positive for BPV produced fibroma in hamsters when given subcutaneously[16] or by scarification[17]. In the present study, we investigated if consumption of the fern *Pteris cretica* and has any influence with Bovine papilloma viruse (BPV) infection in the laboratory model hamster by toxicopathological studies as there are no earlier reports available on this to the best of our knowledge.

Materials and Methods

Collection and processing of fern samples

Pteris cretica was collected from district Nainital, Uttarakhand, India and was shed dried and grounded finely for laboratory animal feeding. The fern sample was identified by the senior Pteridologist Dr. N. Punetha of Pithoragarh, Uttarakhand. Fern sample was analyzed for proximate principles as per[18] at Division of Animal Nutrition of this institute. These were also analyzed for estimation of fern toxin; ptaquiloside (Pta) at Plant and Food Research Institute, Hamilton, New Zealand and flavonoid quercetin at Department of Pharmacognosy, CSIR-National Botanical Research Institute (NBRI), Lucknow for quercetin analysis. Quercetin was estimated in fern samples by thin layer chromatography (TLC). The concentration of Pta and its major breakdown product, pterosin B (PtB), in the fern samples was determined using reversed phase high performance liquid chromatography (HPLC) method[19].

Estimation of quercetin was done as per the method described by Pathania *et al*.[20]. Briefly, 1.0 g of powdered fern sample was extracted with methanol under reflux in a water bath at 100°C. Then it was filtered through Whatman Filter Paper No.1, concentrated and lyophilized. Defatted extract was dissolved in methanol (10 mg/mL) and filtered through 0.45 μM filter and used for quantification of quercetin. TLC was performed on Higlachrosep plates coated with silica (0.2 mm thickness) containing UV 254 fluorescent indicator. 15 μL samples were applied as bands on high performance thin layer chromatography (HPTLC) plate with Hamilton syringes using Linomat 5 applicator (CAMAG). For standard, quercetin (0.5, 1.0 and 1.5 μg/band) was also applied on silica plates. Developing of plates was done in toluene-ethyl acetate-formic acid (7:3:1 v/v/v) in a CAMAG twin-trough chamber. Plates were air dried at room temperature (24°C) and then densitometric scanning was carried out on TLC scanner III using Wincats 3.2.1 software. Phenolic marker plates were scanned and quantified at 400 nm. Using CAMAG Reprostar 3 video documentation unit, images were recorded at 254 and 366 nm. The plates were derivatized in chromatogram immersion device III with anisaldehyde sulphuric acid as reagent, dried and heated at 110°C for 5 min. Then images were taken under visible light.

Preparation of BPV infection material

Cutaneous wart (CW) samples of cattle which were positive for BPV-1 and -2 by PCR were used for preparation of 10% suspension of CWs. Briefly; CW tissues were cleaned, washed, minced with sharp scissors and thoroughly triturated in sterilized pestle and mortar. Then 10% homogenized suspension was prepared in PBS (pH 7.2). The homogenized suspension was subjected to three cycles of freezing and thawing and centrifuged at 12000 rpm for one hour (h). The supernatant was filtered through a 0.45 μM syringe filter. Antibiotics were added and stored at –20°C till further use.

Experimental animals

Syrian golden hamsters of 5-6 weeks age were procured from CSIR-Central Drug Research Institute (CDRI), Lucknow, Uttar Pradesh, India. Animal experiment was approved by the Institutional Animal Ethics Committee as per the rules and regulations of the Committee for the Purpose of Control and Supervision of Experiments on Animals. The hamsters were housed in well ventilated animal house in polypropylene cages. Before start of experiment, animals were acclimatized for 10 days in the experimental shed. The animals were fed with diet formulated in consultation with animal nutritionist.

Experimental design

Twenty four hamsters were divided into four different groups having 6 animals each *viz*. PC, BPV, PC+BPV and C. Animals of PC group were fed with *Pteris cretica* powder @ 15% in standard ration, BPV group given multiple scarifications with 10% CW suspension on skin, PC+BPV group was fed with *P. cretica* powder @ 15% in standard ration along with multiple scarifications with 10% CW suspension on skin and group C was control, fed with standard ration. Duration of the experiment was 28 weeks.

Clinical observations

The animals of different groups were observed daily for the clinical signs, any growth on the site of CW suspension inoculation, respiratory affections,

ocular signs, skin condition, gastro-intestinal disorders and discharges from the natural orifices.

Pathomorphological studies

Gross pathology

At the end of experiment, hamsters were euthanized and systematic necropsy examination was performed. All the internal organs were thoroughly examined for gross lesions and recorded. Skin of all animals was also observed for tumorous growths. The growths were measured with the help of Vernier Callipers.

Histopathology

The representative tissues samples i.e. brain, heart, lungs, liver, spleen, stomach, pancreas, ileum, kidneys, urinary bladder and tumours were preserved in 10% buffered formalin. The paraffin embedded tissues were cut into 4-5-micron thick sections and stained with haematoxylin and eosin (H&E) as per the conventional procedure[21]. Masson's trichrome and toluidine blue staining were done on selected duplicate tissue sections as per standard procedures[22].

Ultrastructural studies

Transmission Electron Microscopy (TEM) studies were carried out on selective target organs *viz*. liver, kidneys, ileum and urinary bladder and tumours developed in animals from various groups at the Electron Microscope Facility, Department of Anatomy, All India Institute of Medical Sciences, New Delhi. For TEM studies, fresh tissue samples were collected from experimental animals and preserved as pieces of 1.0 mm^2 size in 2.5% gluteraldehyde in 0.2 M phosphate buffer (pH 7.4) at 4°C. The tissue pieces were then washed with three changes (2 h each) of cold 0.2 M phosphate buffer (pH 7.4), fixed with 1% osmium tetroxide for 4 h at 4°C, dehydrated in ethyl alcohol, cleared and embedded in epon-araldite resin. Ultra-thin sections were cut by employing ultra microtome (Ultracut Reichert-Jung, Austria) and mounted on copper grids and stained with uranyl-acetate[23] and lead citrate[24]. The sections were washed and allowed to dry on a filter paper in a covered Petri dish at room temperature. The tissue grids were examined under electron microscope at EM Facility (TECNAI G20, FEI Company, Netherland). The samples were screened for suitable areas and ultrastructural images were saved using Soft Imaging Viewer software.

Polymerase chain reaction (PCR)

DNA was extracted from representative tissue samples of skin/tumours using DNeasy Blood and Tissue kit (Qiagen, Hilden, Germany) following manufacturer's protocol and PCR was done to detect presence of BPV. Specific primers[25] targeting the L1 major capsid protein gene of BPV-1 and -2 were used for PCR amplification. These were commercially synthesized from Genetix Biotec. Primers of BPV-1 (forward 5'-GGAGCGCCTGCTAACTATAGGA-3'; reverse 5'-ATCTGTTGTTTGGGTGGTGAC-3') and BPV-2 (forward 5'-GTTATACCACCCAAAGAAGA CCCT-3'; reverse 5'-CTGGTTGCAACAGCTCTCTT TCTC-3') were expected to amplify the specific viral DNA template of sizes 301 and 164 bp, respectively. Thermal profile for PCR reaction was comprised of following steps; initial denaturation step at 94°C for 3 min, followed by step 2 comprised of 35 cycles of denaturation for 40 s at 94°C, annealing for 40 s at 52°C (BPV-1 and -2) with extension at 72°C for 50 s and finally step 3 consisting of a single cycle of final extension at 72°C for 10 min. Amplified DNA fragments were visualized by transillumination under UV light (Geldoc, USA) in 1.5% agarose containing ethidium bromide (0.5 g/mL) as per standard procedures.

Results

Survey and analysis of fern samples

Survey of fern flora was done from different areas in IVRI campus, Mukteswar (2,440 masl), Gas Gadera, Dutkanedhar and near Talla Ramgarh in Nainital district of Uttarakhand. The fern was identified as *Pteris cretica* and found abundant in grazing areas between end of rainy season and onset of winter. It was small bush-like green, semi-green or mature yellow fern, with short or long rhizomes with erect or arching fronds, pinnately divided into 3-5 pairs of linear pinnae. Proximate analysis of fern samples revealed 81.95% dry matter, 8.77% crude protein, 25.06% crude fibre, 1.77% ether extract, 19.59% ash and 9.15% acid insoluble ash. Samples of *Pteris cretica* analyzed for estimation of Pta content revealed that the amount of the toxin was more in green samples as compared to mature dried samples (Table 1). All these samples were tested for presence of quercetin but none was found to contain quercetin.

Clinical observations

Animals from the fern fed group consumed less quantity or sometimes refused to take fern powder

mixed feed in the initial phase of the experiment. Animals of BPV and PC+BPV group revealed presence of small palpable nodules after 11 weeks post inoculation. Subsequently, during 27-28th week post inoculation, all animals from BPV as well as PC+BPV group showed tumours of variable sizes (Fig. 1A, B). However, one animal from PC+BPV group showed multiple tumorous growths (Fig. 1C). During the course of experiment, a total of 3 animals died, 2 from PC and 1 from BPV groups, while no mortality was recorded in animals from control and PC+BPV groups.

Pathomorphological studies

Gross pathology

Tumour description and measurements are presented in Table 2. Grossly, liver from PC and PC+BPV groups showed single to multiple numbers of cysts containing fluids and these were studded in parenchyma (Fig. 2A). Splenomegaly was noticed in animals in PC, BPV and PC+BPV groups and it appeared darker in fern fed groups as compared to control and BPV groups (Fig. 2B). Kidneys from fern

Fig. 1 — Gross appearance of skin at the site of scarification. (A) Ulcerated and haemorrhagic dome shaped growth in a hamster (BPV group); (B) Single sessile, dome shaped growth on hamster skin (PC+BPV group); and (C) Multiple variable shape and sized sessile growths on hamster skin (PC+BPV group) [BPV: Bovine papilloma virus; PC: *Pteris cretica*]

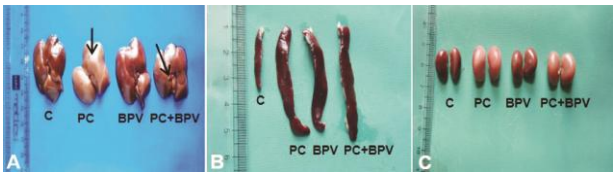

Fig. 2 — Gross changes in liver, spleen and kidneys. (A) Multiple cysts (shown by arrow) studded in liver parenchyma (PC and PC+BPV groups); (B) Splenomegaly (PC, BPV and PC+BPV groups); and (C) Pale and swollen kidneys (PC and PC+BPV groups) [BPV: Bovine papilloma virus; PC: *Pteris cretica*]

Table 1 — Ptaquiloside estimation in *Pteris cretica* from Nainital district of Uttarakhand, India

Source	Place	Toxin (µg/g in dry fern)	
		Pta A +PtB	Pta A
Garden Kraal (Green)	Mukteswar	468.62	332
Garden Kraal (Dried)	Mukteswar	156.68	102
Gas Gadera (Green)	Mukteswar	376.62	349
Gas Gadera (Dried)	Mukteswar	90.56	50
Dutkane Dhar	Ramgarh	817.93	696
Pooled sample	Above places	155.25	93

[Pta A: Ptaquiloside A; PtB: Pterosin B]

Table 2 — Descriptions of tumours with measurements from BPV and *Pteris cretica* + BPV group

Groups	Animals	Gross findings	Tumour dimension (in cms) $d_1 \times d_2 \times h$
BPV	B1	A big oval shaped whitish growth; another peanut sized tumour and several palpable subcutaneous (s/c) nodules	1.5×1.1×0.90
	B2	Scaly skin with alopecia. An irregular round large growth with several (5-6 Nos) palpable s/c nodules	1.54×1.85×1.10
	B3	Two oval to round visible growths and 6-7 palpable s/c nodules	0.35×0.35×0.16 0.40×0.39×0.15
	B4	One small oval shaped and other peanut sized whitish growth	0.20×0.16×0.12
	B5	No visible growth, only 5-6 pin-head to peanut sized palpable nodules	-
PC + BPV	BP1	One big dome shaped whitish growth; two small visible peanut sized growths and several nodule-like palpable structures	1.43×1.20×0.62
	BP2	Scaly and thickened skin. One big oval shaped whitish growth, six small peanut sized visible growths and several (6-7 Nos) palpable nodules	0.74×0.85×0.50
	BP3	A number of variable shaped, spherical, oval, round and irregular sized growths on dorsal surface and several other palpable nodules in adjoining areas	1.15×1.19×0.70 0.66×0.64×0.35 0.50×0.50×0.23 0.50×0.75×0.26 0.60×1.16×0.21 0.61×0.52×0.20
	BP4	No visible growth, only several variable sized palpable subcutaneous nodules were detected	-
	BP5	One big visible growth and other peanut sized palpable nodules were detected	0.72×0.74×0.29
	BP6	Three growths, one pin-head and two peanut sized visible growths and several variable sized palpable subcutaneous nodules were detected	0.25×0.29×0.16 0.21×0.23×0.18

[BPV: Bovine papilloma virus; PC: *Pteris cretica* d_1 and d_2: Diameters of tumorous growth; h: Height of tumorous growth above the skin surface]

fed groups were swollen and pale in colour as compared to control and BPV groups (Fig. 2C). Small intestine of one animal from PC+BPV groups showed serosal haemorrhages at the level of Peyer's patches.

Histopathology

Details of histopathological lesions observed in different groups are presented in Table 3.

PC group

Animals revealed mild engorgement of blood vessels in brain, focal areas of emphysema and atelectasis in lungs, cloudy swelling of hepatocytes with granular cytoplasm, blood vessels were dilated and focal mononuclear cells (MNCs) infiltration, occasionally Kupffer cell proliferation and bile duct hyperplasia with formation of juvenile bile ducts at some foci. Single to multiple cysts were observed in hepatic parenchyma surrounded by MNCs infiltration (Fig. 3A). In the areas surrounding central veins necrosis of hepatocytes with pyknotic nuclei was evident. Spleen showed pronounced haemorrhages with presence of haemosiderin pigment and focal areas of necrosis in white pulp (Fig. 3B). Sloughed off villi with lining epithelial cells and engorgement of blood capillaries/vessels in mucosa as well as in submucosa (Fig. 3C), prominent goblet cells in the lining epithelium of villi and prominent Peyer's patches were observed in ileum. Occasionally, denudation of mucosal epithelium and MNCs infiltration was also noticed. Pancreas showed

Table 3 — Histopathological changes in various organs of hamsters after *Pteris cretica* feeding and its association with BPV at 28 weeks

Organs	Lesions	Groups			
		PC	BPV	PC+ BPV	Control
Brain	Engorged vasculature	2/6	0/6	2/6	0/6
	Oedema	1/6	0/6	1/6	0/6
Heart	Engorged vasculature	0/6	1/6	1/6	0/6
Lungs	Engorged alveolar capillaries	3/6	1/6	6/6	2/6
	Focal emphysema and atelectasis	6/6	6/6	6/6	3/6
	Bronchial epithelial desquamation	0/6	0/6	1/6	0/6
	Corpora amylacea	1/6	0/6	1/6	0/6
Liver	Engorged vasculature	4/6	2/6	4/6	2/6
	Hepatocytic degeneration	2/6	0/6	3/6	0/6
	Bile duct hyperplasia	4/6	1/6	6/6	0/6
	Cystic wall pressure degeneration	3/6	0/6	5/6	0/6
	Perivascular MNCs infiltration	4/6	2/6	5/6	1/6
	Hepatic necrosis	2/6	1/6	3/6	0/6
Spleen	Haemorrhages /haemosiderosis	2/6	0/6	4/6	0/6
	Degenerative changes	1/6	1/6	2/6	0/6
	Necrosis	2/6	0/6	2/6	0/6
	Splenic protrusion	0/6	2/6	0/6	0/6
Glandular Stomach	Engorged vasculature	3/6	2/6	4/6	0/6
	Denudation of mucosal epithelium	1/6	0/6	0/6	0/6
	MNCs infiltration	1/6	0/6	1/6	0/6
Non-glandular Stomach	Engorged vasculature	1/6	0/6	1/6	0/6
	MNCs infiltration	0/6	0/6	2/6	0/6
Ileum	Engorged vasculature	3/6	1/6	3/6	0/6
	Sloughed off/distorted/necrosis of villi	2/6	0/6	2/6	0/6
	Goblet cells hyper activity	2/6	1/6	3/6	0/6
	Prominent Peyer's patches	3/6	0/6	4/6	0/6
Kidneys	Engorged vasculature	4/6	3/6	5/6	2/6
	Tubular dilatation with eosinophilic cast	3/6	2/6	4/6	0/6
	Tubular epithelium degeneration	3/6	0/6	4/6	0/6
Urinary bladder	Engorged vasculature	4/6	4/6	4/6	2/6
	Focal urothelial hyperplasia	1/6	0/6	2/6	0/6
	Nuclear atypia	0/6	1/6	0/6	0/6
	Oedema	0/6	1/6	2/6	0/6
	MNCs infiltration	0/6	1/6	2/6	0/6

[Scoring: Number of organs showing lesions/number of organs examined (n = 6 hamsters/group), MNCs: Mononuclear cells]

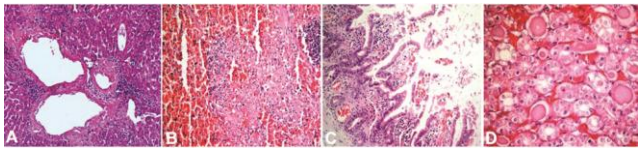

Fig. 3 — Histopathological changes in haematoxylin and eosin (H&E) stained sections of liver, spleen, ileum and kidney. (A) Cysts in hepatic parenchyma surrounded by MNCs infiltration (PC group). H&E×100; (B) Pronounced haemorrhages and focal area of necrosis in spleen (PC group). H&E×200; (C) Engorgement of blood vessels and disrupted mucosa and submucosa in ileum (PC group). H&E×200; and (D) Engorgement of blood vessels and eosinophilic casts in lumina of renal tubules (PC group). H&E×400 [PC: *Pteris cretica*]

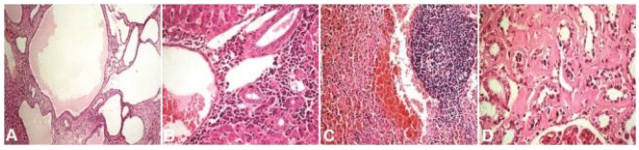

Fig. 4 — Histopathological changes in haematoxylin and eosin (H&E) stained sections of liver, spleen and kidney. (A) Cystic wall showing necrosis and MNCs infiltration in hepatic parenchyma (PC+BPV group). H&E×200; (B) Bile duct hyperplasia admixed with MNCs infiltration (PC+BPV group). H&E×400; (C) Massive haemorrhages surrounding splenic white pulp (PC+BPV group). H&E×100; and (D) Renal cortex showing homogenous eosinophilic renal tubules with degenerative changes in lining epithelium (PC+BPV group). H&E×400 [BPV: Bovine papilloma virus; PC: *Pteris cretica*]

multilocular cysts. Kidneys showed engorgement of blood vessels and hypertrophied glomeruli with reduction of Bowman's space. In medulla renal tubules showed the presence of eosinophilic casts (Fig. 3D). Urinary bladder revealed mild engorgement of blood vessels in lamina propria and focal areas of urothelial denudation.

BPV group

Hamsters showed mild vascular changes in heart, lungs, liver, stomach and kidneys. Liver revealed focal areas of MNCs infiltration in perivascular areas in two animals and bile duct hyperplasia was seen in one case. Spleen from two animals showed depletion of white pulp and organized fibrinous protrusion on splenic capsule. Ileum showed hypersecretory activity with prominent goblet cells in one case. Occasionally, urothelium showed hyperchromatic nuclei with nuclear atypia.

PC + BPV group

In PC+BPV group, brain showed mild engorgement of blood vessels in two animals while oedema in one animal. Myocardium from one animal showed engorgement of blood vessels and lungs showed atelectasis and engorgement of alveolar blood capillaries. Focal areas of desquamation of bronchial epithelium and occasionally, corpora amylacea were evident in the lung parenchyma. Liver showed swollen hepatocytes with granular cytoplasm and mid-zonal vacuolar degenerative changes. It revealed numerous cysts lined with cuboidal epithelium surrounded by areas of necrosis with moderate to intense focal MNCs infiltration in pericystic, perivascular areas or in parenchyma (Fig. 4A). Bile duct hyperplasia with newly formed non-functional bile ducts with MNCs infiltration was observed (Fig. 4B). Spleen showed marked haemorrhages (Fig. 4C), degenerative changes and focal necrotic areas in white pulp. Mucosal layer of stomach showed engorgement of blood vessels with erythrocytes. Lamina propria of non-glandular stomach showed mild infiltration with MNCs. Pancreas from two animals revealed unilocular to multilocular cysts. Ileum revealed goblet cell proliferation with excessive mucus secretion. Peyer's patches showed marked proliferation. Destruction of villi, plasma cell infiltration and haemosiderosis were also evident in ileum. Kidneys showed shrunken glomeruli with marked Bowman's spaces. Glomerular capillaries as well as blood vessels in cortico-medullary areas were engorged. Renal tubules of cortical area showed degenerative changes (Fig. 4D) and presence of few eosinophilic casts.

Control group

The lung showed focal areas of emphysema and atelectasis in three cases, occasionally MNCs infiltration in liver, mild engorgement of blood vessels at cortico-medullary junction of kidneys and urinary bladder. No microscopic changes were seen in brain, heart, spleen, stomach, intestine and skin.

Tumours

Experimental hamsters from BPV groups showed growths on the skin. Histopathologically, these were characterized by hyperkeratosis with thickening of stratum corneum and proliferative masses of fibroblasts and fibrocytes of variable sizes, arranged in different directions (Fig. 5A). Few animals also revealed excessive thickening of stratum spinosum with well developed rete pegs and round to oval proliferating lipocytes in tumour stroma. Focal area of necrosis with MNCs infiltration was observed. Nuclear crowding was evident in infiltrating areas. Tumour stroma from majority of cases showed mild to moderate infiltration of mast cells. These tumours were diagnosed as fibroma and lipofibroma with more

specifically low grade fibrosarcoma. Duplicate sections of tumours were stained with Masson's trichrome revealed proliferating spindle shaped fibroblasts with abundant collagen (stained bluish) and overlying epidermis (stained reddish) (Fig. 5B).

In PC+BPV group, the tumours were well circumscribed with encapsulation. Epidermis was intact in all cases with variable features of either thinning or thickening along with excessive cornification and formation of well-developed rete pegs (Fig. 5C). Collagen fibres were repetitive and usually arranged in interwoven fascicles and in whorl pattern. In all cases, there was proliferation of loose connective tissue followed by an underlying mass of proliferating fibrocytes and fibroblasts of different sizes with pleomorphic (oval, elongated or spindle shaped) hyperchromatic and vesicular nuclei and arranged in different directions**.** In two cases, the neoplastic fibrous connective tissues grown beyond muscularis layer and in between proliferating lipocytes were also seen. These proliferating lipocytes were of variable size and some were fused together. In all cases, sebaceous glands had undergone degeneration leaving remnants. Proliferation of skin adenaxes mainly hair follicles were evident in three cases. In some cases, focal necrotic areas with MNCs (lympho-plasmocytic) infiltration were seen. Tumour stroma from majority of cases showed mild to moderate infiltration of specific large cells with hyperchromatic nuclei and granular cytoplasm. Toluidine blue staining confirmed these cells as mast cells (Fig. 5D). These tumours were diagnosed as fibroma and lipofibroma with more specifically low grade fibrosarcoma.

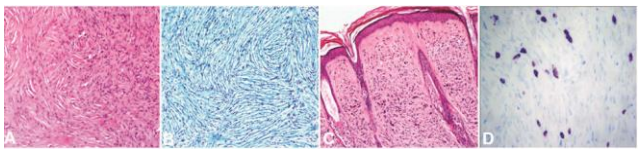

Fig. 5 — Histopathological changes in haematoxylin and eosin (H&E) stained sections of skin tumours. (A) Proliferative masses of fibroblasts and fibrocytes of variable sizes arranged in different directions. Fibroma, BPV group, H&E×200; (B) Proliferating spindle shaped fibroblasts with abundant collagen (stained bluish) and nuclei (stained blackish). Fibroma, BPV group, Masson's Trichrome×200; (C) Tumour mass encapsulated with overlying stratum corneum and thin epidermis with rete pegs inserted into proliferating fibrous connective tissue admixed with hyperchromatic mast cells. Fibroma, PC+BPV group, H&E×100; and (D) Tumour stroma showing mast cells (stained reddish-purple) and background (stained bluish). Fibroma, PC+BPV group, Toluidine Blue ×400 [BPV: Bovine papilloma virus; PC: *Pteris cretica*]

Ultrastructural pathology

PC group

Hepatocytes had round nuclei with damaged double walled nuclear membrane, margination of nucleolus and electron dense or semi-lucent variable sized swollen mitochondria with indistinct cristae in cytoplasm (Fig. 6A). Enterocytes had numerous microvilli and cytoplasm with numerous mitochondria of variable shapes and sizes (Fig. 6B). In some of these enterocytes, mitochondria appeared to be dividing and, in many others, the mitochondrial membrane was indistinct and damaged at various places. In some other areas, enterocytes were present with distinct cytoplasmic membranes, cell junctions and these looked like communicating channels with each other. It also showed presence of a number of electron light goblet-like secretory cells composed of multiple lobulations. Renal tubular cells had round

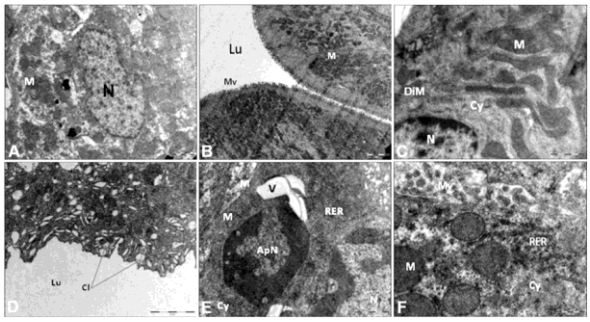

Fig. 6 — Ultrastructural changes on transmission electron microscopy in tissues from liver, ileum, kidney and urinary bladder. (A) Liver: Hepatocyte with part of nucleus (N) with damaged nuclear membrane. Cytoplasm is showing fused electron dense variable size mitochondria (M) with indistinct cristae. PC group, TEM×1600; (B) Ileum: Surface of ileum facing lumina (Lu) showing enterocytes with abundance of cytoplasm studded with numerous mitochondria (M). Mucosal lining is having numerous microvilli (Mv) facing luminal surface. PC group, TEM×2000; (C) Kidney: Renal tubular epithelial cell with part of nucleus (N) and abundance of cytoplasm (Cy) showing numerous electron dense elongated tubular mitochondria (M) with a few damaged mitochondria (DiM). PC group, TEM×5000; (D) Urinary bladder: The mucosa of the urinary bladder facing the lumina (Lu) showed scalloped appearance and numerous cleft (Cl) like structures. PC group, TEM×3200; (E) Liver: Oval shaped apoptotic nucleus (ApN) with prominent marginated heterochromatin and nucleus of adjoining cell showed nuclear changes of less intensity. Cytoplasmic details are not clear except presence of few mitochondria (M), rough endoplasmic reticulum (RER) and a slit-like large vacuole (V) close to nuclear membrane. BPV group, TEM×5000; and (F) Liver: Cytoplasm (Cy) showed multiple electron dense mitochondria (M), scanty RER and microvilli (Mv) on cytoplasmic membrane and interstitial space. PC+BPV group, TEM×8000 [BPV: Bovine papilloma virus; PC: *Pteris cretica*]

nuclei and abundance of cytoplasm. Occasionally, apoptotic nucleus with margination of heterochromatin was seen. Cytoplasm contained variable shaped (oval/elongated/dumble) electron dense mitochondria (Fig. 6C) and these were surrounded by variable length tubular rough endoplasmic reticulum (RER) like structures. Urothelium showed luminal surface with electron dense scaffold-like structures facing to lumina and additionally, it had several cleft-like and vacuolar spaces (Fig. 6D). Urothelial cells contained abundance of cytoplasm and pleomorphic nuclei (round, oval, elliptical or irregular). Cytoplasm was semi-lucent and revealed abundance of mitochondria. Cisternae of RER were dilated. Intercellular spaces were not prominent and few tight junctions were also present. At places, abundance of collagen fibres were observed. Blood capillaries containing RBCs were also seen.

BPV group

Hepatocytes revealed round nuclei and centrally or perimarginally placed nucleolus. Cytoplasm contained abundance of electron dense mitochondria with indistinct cristae and plenty of RER. In some hepatocytes oval shaped apoptotic nuclei with prominent marginated heterochromatin was also observed. Adjoining cell nuclei showed less intensity of nuclear changes. Cytoplasmic details were not clear except few mitochondria and a slit-like large vacuole close to nuclear membrane (Fig. 6E). Enterocytes surface facing lumina had a dense zone of microvilli and contained round to oval nuclei with abundance of cytoplasm. Renal tubular cells contained cells with oval nuclei, abundance of cytoplasm and variable sized electron dense mitochondria. Some mitochondria were very close to the periphery of nuclei with few microtubular structures adjoining to mitochondria.

PC+BPV group

Hepatocytes showed occasionally nucleoplasmolysis and apoptotic nuclei with condensation of heterochromatin at margins of the nucleus. Cytoplasm showed numerous electron dense variable shaped (oval or elongate) swollen mitochondria, electron dense vesicular structures, RER and few vacuoles (Fig. 6F). Enterocytes showed dense zone of microvilli and degenerating enterocytes with pleomorphic nuclei and cytoplasmolysis. Prominent vacuolating spaces were seen around nuclei with clumping of cytoplasm (Fig. 7A). Renal tubular cells

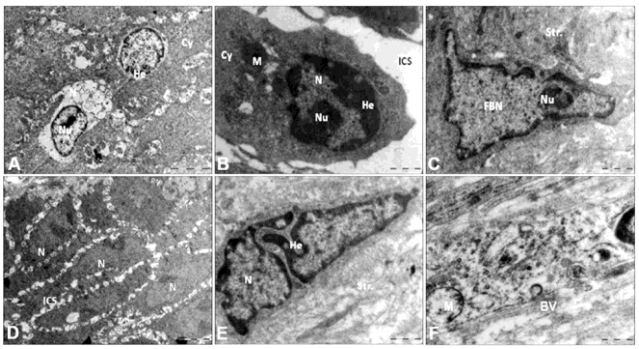

Fig. 7 — Ultrastructural changes on transmission electron microscopy in tissues from ileum, kidney and tumours. (A) Ileum: Variable shaped nuclei (N) with electron dense nucleolus (Nu) placed marginally or at centre. The cytoplasmic (Cy) details are not distinct. PC+BPV group, TEM×1000; (B) Kidney: Apoptotic nucleus (N) with condensation, margination of heterochromatin (He) and perimarginally placed nucleolus (Nu). Cytoplasm (Cy) is plenty, electron dense with presence of a few mitochondria (M) and vacuoles. Intercellular space (ICS) is prominent. PC+BPV group, TEM×4000; (C) Tumour: Fibroblast with triangular shaped elongated nucleus (FBN) with scanty cytoplasm. Its nucleolus (Nu) is prominent and marginally placed heterochromatin and unidentified structure (str). Fibroma, BPV group, TEM×4000; (D) Tumour: Variable shaped fibroblasts with scanty cytoplasm and numerous microvilli on its surface and prominent intercellular spaces (ICS). Fibroma, PC+BPV group, TEM×2000; (E) Tumour: Binucleated fibroblast with prominent heterochromatin (He) arranged along the margins of nucleus (N). Cytoplasm is scanty with indistinct cell membranes and devoid of cell organelles. Fibroma, PC+BPV group, TEM×4000; and (F) Tumour: Cytoplasm with ribosomes, mitochondria and some round budding virus-like (BV) particles seen on cytoplasmic membranes. Fibroma, PC+BPV group, TEM×8000 [BPV: Bovine papilloma virus; PC: *Pteris cretica*]

revealed round to oval shaped nuclei and abundance of cytoplasm with a tendency of electron dense in nature. Occasionally, few cells showed apoptotic nuclei with perimarginally placed enlarged nucleolus (Fig. 7B).

Tumours

BPV group

Tumour cells revealed fibroblasts with abundance of collagen fibres. Fibrocytes had elongated nuclei with the tapering end of cytoplasmic processes. Occasionally, fibroblasts had triangular shaped elongated nuclei with scanty cytoplasm and unidentified structure. Its nucleolus was prominent with margination of heterochromatin (Fig. 7C). A few other cells contained oval or irregular shaped nuclei with smaller, oval to round electron dense structures (histamine granules) with indistinct membranes in their cytoplasm. These areas also contained electron dense disrupted RER. In some other areas, apoptotic

cells were seen which showed cytoplasmolysis and certain unidentified membranous structures on cytoplasmic membranes.

PC+BPV group

Tumour growth showed variable shaped fibroblasts with prominent intercellular spaces (Fig. 7D). The tumour stroma was comprised of fibroblasts with pleomorphic nuclei and abundance of collagen fibres. It also showed few fibrocytes and a binucleated fibrocyte. Latter had prominent heterochromatin which was arranged along the margins of nucleus. Fibroblasts had scanty cytoplasm with indistinct cell membranes (Fig. 7E). These cells had electron dense organelle. Cytoplasm of these cells had RER with dilated cisternae, few vesicular structures and cross section of few microtubules. Some round budding virus-like particles were also seen on cytoplasmic membranes (Fig. 7F).

PCR

DNA was extracted from the tumour/skin samples collected from hamsters of different groups; PC, BPV, PC+BPV and control. Tumour samples from BPV and PC+BPV groups were positive for DNA of BPV-1 and -2 while in none of the samples from PC and control groups DNA of BPVs were detected.

Discussion

There are many ferns which are known to contain toxins. The toxin, ptaquiloside (Pta) is the most abundant in some ferns. Similarly, this toxin was also present in *Pteris cretica.* In present study, toxicopathological effects of *P. cretica* feeding and its association with BPV was assessed in hamsters. Most of the experimental studies have been performed on bracken fern and other non-bracken ferns-like *Onychium contiguum* Wall. ex Hope, *Dryopteris juxtaposita* H. Christ, *Cheilanthes farinosa* Kaulf etc. Despite our best efforts with literature search, we could not find any experimental study performed on *P. cretica*-BPV infection in laboratory model hamster. This study was undertaken because *P. cretica* had many times high level of toxin than any other fern. In the present study, Pta content (Pta A + Pta B) and Pta A (µg/g dry fern powder) in *P. cretica* was variable, from different sources it ranges from 90.56 to 817.93 and 50.0 to 696.0, respectively. However, none of the samples showed the presence of quercetin. Proximate analysis revealed that crude protein and ether extract levels were comparable to great extent to *Polystichum* and *Dryopteris*, however, the values of total ash and acid insoluble ash were higher than *Dryopteris*, *Cheilanthes*, *Bracken* and *Polystichum* as reported by earlier workers[26].

Experimental hamsters preferred fresh feed and initially their feed intake was reduced due to 15% fern in their ration but later it became normal. Similar behavioural findings were reported earlier also. Animals from BPV and PC+BPV group showed the development of tumours of variable sizes during the progression of the experiment. The present findings are in corroboration with that of reported by earlier workers[17,27].

Histopathologically, the animals from PC group showed mild congestion in brain, cloudy swelling, bile duct hyperplasia and perivascular necrosis in liver and prominent red pulp and depleted white pulp in spleen. Animals from BPV groups showed mild vascular changes in heart, lungs, liver, stomach, kidneys and urinary bladder. Animals from PC+BPV group showed vascular changes in brain, heart, lungs, liver, stomach, ileum, kidneys and urinary bladder. Liver showed hepatocytes with vacuolar and granular degenerative changes, moderate to intense focal perivascular MNCs infiltration, bile duct hyperplasia with newly formed non-functional bile ducts and numerous cysts lined with cuboidal epithelium. Spleen showed pronounced haemorrhages. Hypersecretory activity with prominent goblet cells in lining epithelium of villi in the intestine was observed. Kidneys showed shrunken glomeruli with marked Bowman's spaces, engorged glomerular capillaries and blood vessels, degenerative changes with presence of few eosinophilic casts in renal tubules of cortical region. Similar to present study, mild to moderate vascular changes in most of the visceral organs, vacuolar degenerative changes in hepatocytes, hypersecretory activity in intestine, presence of casts in renal tubules and degenerative changes in the renal tubular lining epithelial cells were observed by earlier workers in rabbits[28], rats[29,30] and hamsters[17]. Some of later findings were suggestive of renal impairment due to fern feeding and were comparable to those observed in various fern toxicity studies[31,32]. However, no reports on the toxicity of *P. cretica* in hamsters are available in literature, as such for the first time its toxicity was proved. The *P. cretica* fern was found to be hepatotoxic and nephrotoxic.

Ultrastructurally, liver and kidney from PC group showed degenerative changes. These were

characterized by margination of nucleolus, cytoplasm with either electron dense or semi-lucent variable sized swollen mitochondria with indistinct cristae and indistinct RER with dilated cisternae. Ileum showed enterocytes with abundant cytoplasm studded with numerous mitochondria of variable shapes (elongated/oval/dumble) and sizes. Similar findings were also observed in PC+BPV group. BPV group showed less degree of degenerative changes. Scanty information is available on ultrastructural changes produced in liver, ileum, kidney and urinary bladder due to effects of BPV and fern association. The ultrastructural changes observed in these organs were more or less similar to that reported in experimental rats fed with *Pteris cretica*[30,33]. Somvanshi and Singh[34] reported degenerated nuclear wall, vacuolations, certain electron dense inclusions and degenerated mitochondria, fusiform vesicles and prominent intercellular spaces in cytoplasm of urinary bladder cells in *Polystichum* fed guinea pigs.

BPV and PC+BPV groups developed variable sized raised and palpable nodular growths similar to previous reports where these growths revealed proliferation of fibrocytes and fibroblasts of variable nuclei (oval, elongated or spindle shaped), eosinophilic mature collagen fibres arranged haphazardly in different directions with whirling pattern. The skin tumours induced in hamsters in present study were in accordance with the studies by earlier workers[17,27,35]. Somvanshi *et al*.[35] reported tumours developed in hamsters as fibrosarcomas of low-grade malignancy without metastasis. Singh *et al*.[27] reported that the skin of hamsters revealed different stages of pre-neoplastic to early neoplastic, ranging from proliferation and thickened zone of collagen and reticulin fibres in the sub epidermal layer to proliferative changes in hypodermal fibroblasts and lipocytes leading to conditions like fibroplasia, fibroma and lipofibroma. The findings were similar to the earlier reports of progressing fibromas, fibromas and fibroblastic tumours induced by inoculation of cattle CWs[27,36].

In present study, there was no development of tumours in ileum and urinary bladder. Contrary to present study, different levels of added Pta chemical induced ileal and bladder tumours in rats[9], gastric tumours in mice[37], transitional cell carcinoma and adenocarcinoma in urinary bladder of guinea pigs[32]. In present study, almost all hamsters from BPV and PC+BPV groups showed either single or double large-sized tumorous growths. But, in one hamster from PC+BPV group multiple (6 Nos.) tumorous growths were observed. However, the animals revealed development of multiple subcutaneous nodules at the site of scarification. Our findings suggest that there were only negligible to mild effects of *P. cretica*-BPV infection on tumour development in experimental animals. Ultrastructurally, tumour cells from BPV group revealed that the stroma was comprised of fibroblasts with variable shaped (oval to elongate) enlarged nuclei and scanty cytoplasm. However, some other cells were pleomorphic (fibroblasts and fibrocytes). Occasionally, in few cells, nucleolus was marginal. A few cells were binucleated with presence of electron dense granules and in other cells, nuclei were indistinct and cytoplasm showed a tendency of electron dense in nature. Cytoplasm of these cells contained degenerated mitochondria, numerous variable sized vacuoles, few electron dense oval shaped phagolysosomes and numerous microtubules. Tumour cells of PC+BPV group also showed similar ultrastructural features. It is reported that the well differentiated fibrosarcoma reveal uniform spindle shaped fibroblastic cells separated by variable number of collagenous fibrils[38,39].

In present study, PCR was carried on DNA extracted from tumour/skin samples of the animals from different groups; PC, BPV, PC+BPV and control. It revealed the presence of DNA of BPV-1 and -2 in samples from BPV and PC+BPV groups. In none of the samples from PC and control groups, DNA of BPVs were detected. This indicated that the BPVs in hamsters from BPV and PC+BPV groups induced the cellular proliferation which lead to development of visible growths. These observations were similar to earlier workers[17,40].

Conclusion

Observations from the present study showed that non-bracken fern species, *Pteris cretica* from Uttarakhand contain moderate amount of Pta toxin. In the initial days of experiment, feed intake was reduced in fern fed hamsters but later on became normal. Variable sized tumours developed in the hamsters from BPV and PC+BPV groups during the progression of experiment. In fern fed groups, hamsters revealed important pathological lesions mainly in liver and kidneys. Liver revealed degenerative changes in hepatocytes, moderate to intense infiltration of mononuclear cells in focal

perivascular areas, bile duct hyperplasia and numerous cysts. Degenerative changes, shrunken glomeruli and congestion were noticed in kidneys. The toxicopathological effects of the fern in liver and kidneys revealed that this fern is hepatotoxic and nephrotoxic in hamsters. In fern fed groups (PC, PC+ BPV), ileum of hamsters showed prominent goblet cells and Peyer's patches. Spleen of hamsters from these groups also revealed haemorrhages and haemosiderosis. Association between *Pteris cretica* and BPV infection was negligible to mild but long-term studies are required. Consumption of *P. cretica* alone or in combination with *P. aquilinum* (bracken fern) or Onychium species by grazing cattle of hilly tract in scarcity period may lead to serious threat for these animals.

Acknowledgement

Authors acknowledge Dr S Khatoon for estimating quercetin in fern samples. The first author is grateful to the Indian Council of Agricultural Research, New Delhi for financial assistance in the form of a scholarship.

Conflict of interest

Authors declare no conflict of interests.

References

1 de Winter WP & Amoroso VB, *Plant Resources of South-East Asia*. (Backhuys Publishers, Leiden), 2003, 167.

2 Saito K, Nagao T, Takatsuki S, Koyama K & Natori S, The sesquiterpenoid carcinogen of bracken fern and some analogues from the Pteridaceae. *Phytochemistry*, 29 (1990) 1475.

3 Recouso RC, Stocco dos Santos RC, Freitas R, Santos RC, de Freitas AC, Brunner O, Becak W & Lindsey CJ, Clastogenic effect of bracken fern (*Pteridium aquilinum v. arachnoideum*) diet in peripheral lymphocytes of human consumers: preliminary data. *Vet Comp Oncol*, 1 (2003) 22.

4 Ferguson LR & Philpott M, Nutrition and mutagenesis. *Annu Rev Nutr*, 28 (2008) 313.

5 Tourchi-Roudsari M, Multiple effects of bracken fern under *in vivo* and *in vitro* conditions. *Asian Pac J Cancer Prev*, 15 (2014) 7505.

6 Kisielius V, Lindqvist DN, Thygesen MB, Rodamer M, Hansen HCB & Rasmussen LH, Fast LC-MS quantification of ptesculentoside, caudatoside, ptaquiloside and corresponding pterosins in bracken ferns. *J Chromatogr B*, 1138 (2020) 121966.

7 Rai SK, Sharma R, Kumari A, Rasmussen LH, Patil RD & Bhar R, Survey of ferns and clinico-pathological studies on the field cases of enzootic bovine haematuria in Himachal Pradesh, a north-western Himalayan state of India. *Toxicon*, 138 (2017) 31.

8 Smith BL, Seawright AA, Ng JC, Hertle AT, Thomson JA & Bostock PD, Concentration of ptaquiloside, a major carcinogen in bracken fern (*Pteridium* spp.) from eastern Australia and from a cultivated worldwide collection held in Sydney, Australia. *Natural Toxins*, 2 (1994) 347.

9 Hirono I, Ogino H, Fujimoto M, Yamada K, Yoshida Y, Ikagawa M & Okumura M, Induction of tumors in ACI rats given a diet containing ptaquiloside, a bracken carcinogen. *J Natl Cancer Inst*, 79 (1987) 1143.

10 Bjeldanes LF & Chang GW, Mutagenic activity of quercetin and related compounds. *Science*, 197 (1977) 577.

11 Pangty K, Singh S, Saikumar G, Goswami R & Somvanshi R, Detection of BPV-1 and -2 and quantification of BPV-1 by real-time PCR in cutaneous warts in cattle and buffaloes. *Transbound Emerg Dis*, 57 (2010) 185.

12 Russo V, Roperto F, de Biase D, Cerino P, Urraro C, Munday JS & Roperto S, Bovine papilloma virus type 2 infection associated with papillomatosis of the amniotic membrane in water buffaloes (*Bubalus bubalis*). *Pathogens*, 9 (2020) 262.

13 Bam J, Kumar P, Leishangthem GD, Saikia A & Somvanshi R, Spontaneous cutaneous papillomatosis in yaks and detection and quantification of bovine papillomavirus -1 and -2. *Transbound Emerg Dis*, 60 (2013) 475.

14 Tsirimonaki E, O'Neil BW, Williams R & Campo MS, Extensive papillomatosis of the bovine upper gastrointestinal tract. *J Comp Pathol*, 129 (2003) 93.

15 Campo MS, Jarrett WFH, Barron R, O'Neill BW & Smith KT, Association of bovine papilloma v*irus type 2* and bracken fern with bladder cancer in cattle. *Cancer Res*, 52 (1992) 6898.

16 Pfister H, Fink B & Thomas C, Extrachromosomal bovine papilloma virus type 1 DNA in hamster fibromas and fibrosarcomas. *Virology*, 115 (1981) 414.

17 Leishangthem GD, Somvanshi R & Lauren DR, Pathological studies on Bovine papilloma virus-fern interaction in hamsters. *Indian J Exp Biol*, 46 (2008) 100.

18 AOAC, *Official Methods of Analysis*, (Association of Official Analytical Chemists, Washington, DC, USA), 1995.

19 Agnew MP & Lauren DR, Determination of ptaquiloside in bracken fern (*Pteridium esculentum*). *J Chromatogr*, 538 (1991) 462.

20 Pathania S, Kumar P, Singh S, Khatoon S, Rawat AKS, Punetha N, Jensen DJ, Lauren DR & Somvanshi R, Detection of ptaquiloside and quercetin in certain Indian ferns. *Curr Sci*, 102 (2012) 1683.

21 Culling CFA, *Hand book of Histopathological and Histochemical Techniques*, (Butterworths, London), 1974, 193.

22 Luna LG, *Manual of Histological Staining Methods of the Armed Force Institute of Pathology*, (Mc Graw-Hill Book Company, London), 1968, 94.

23 Watson ML, Staining of tissue sections for electron microscopy with heavy metals. *J Biophys Biochem Cytol*, 4 (1958) 475.

24 Reynolds ES, The use of lead citrate at high pH as an electron opaque stain in electron microscopy. J Cell Biol, 17 (1963) 208.

25 Yaguiu A, de Carvalho C, de Freitas AC, Goes LGB, Dagli MLZ, Brigel Jr EH, Becak W & de Cassia Stocco dos Santos R, Papillomatosis in cattle: *In situ* detection of bovine papillomavirus DNA sequences in reproductive tissues. *Braz J Morphol Sci*, 23 (2006) 525.

26 Senger SS & Somvanshi R, Chemical profile of some ferns. *Indian Fern J*, 17 (2000) 106.

27 Singh V, Somvanshi R & Tiwari AK, Papillomatosis in Indian cattle: occurrence and etiopathology. *Indian J Vet Pathol*, 33 (2009) 52.

28 Gounalan S, Somvanshi R, Kataria M, Bisht GS, Smith BL & Lauren DR, Effect of bracken (*Pteridium aquilinum*) and dryopteris (*Dryopteris juxtaposita*) fern toxicity in laboratory rabbits. *Indian J Exp Biol*, 37 (1999) 980.

29 Gounalan S, Somvanshi R, Kumar R, Dash S & Devi V, Clinico-pathological effects of bracken fern (*Pteridium aquilinum*) feeding in laboratory rats. *Indian J Anim Sci*, 69 (1999) 385.

30 Sreelekshmy M & Somvanshi R, Evaluation of toxicopathological effects of *Pteris cretica* in laboratory rats. *Vegetos Int J Plant Res*, 29 (2016) 87.

31 Sivasankar S & Somvanshi R, Pathological evaluation of *Polystichum squarrosum* (D. Don) fern in laboratory rats. *Indian J Exp Biol*, 39 (2001) 772.

32 Dawra RK, Kurade NP & Sharma OP, Carcinogenicity of the fern *Pteridium aquilinum* collected from enzootic bovine haematuria-free hilly area in India. *Current Sci*, 83 (2002) 1005.

33 Sreelekshmy M, *Molecular detection of bovine papilloma virus types associated with papillomatous lesions in large animals and toxicopathological effects of Pteris cretica in rats*, M.V.Sc. thesis, Deemed University, Indian Veterinary Research Institute, Izatnagar, Uttar Pradesh, 2014.

34 Somvanshi R & Singh AK, Transmission electron microscopic studies of urinary bladder in *Polystichum squarrosum* fern fed guinea pigs. *Indian J Vet Pathol*, 29 (2005) 27.

35 Somvanshi R, Iyer PKR, Sharma B, Koul GL & Biswas JC, Transmission studies on bovine cutaneous papillomas in hamsters. *Indian J Anim Sci*, 58 (1988) 752.

36 Lancaster WD & Olson C, Animal papillomaviruses. *Microbiol Rev*, 46 (1982) 191.

37 Evans IA & Galpin OP, Bracken and leukaemia. *Lancet*, 335 (1990) 231.

38 Antonescu CR & Baren A, Spectrum of low-grade fibrosarcomas: a comparative ultrastructure analysis of low-grade myxofibrosarcoma and fibromyxoid sarcoma. *Ultrastruct Pathol*, 28 (2004) 321.

39 Enzinger FM & Weiss SW, *Soft Tissue Tumours*, (St. Louis CV, Mosby), 2001, 411.

40 Kumar P, *Etiopathological characterization of cutaneous and mucosal warts of cattle and buffaloes and experimental studies on interaction of quercetin with BPV and DMBA induced tumours in hamsters*, (Ph.D. thesis, Deemed University, Indian Veterinary Research Institute, Izatnagar, Uttar Pradesh), 2012.